www.nature.com/aps

Acta Pharmacologica Sinica

ARTICLE

# β-Arrestin2 deficiency attenuates oxidative stress in mouse hepatic fibrosis through modulation of NOX4

Jia-jia Du[1], Jia-chang Sun[1], Nan Li[1], Xiu-qin Li[1], Wu-yi Sun[1] and Wei Wei[1]

Hepatic fibrosis is a disease characterized by excessive deposition of extracellular matrix (ECM) in the liver. Activation of hepatic stellate cells (HSCs) is responsible for most of ECM production. Oxidative stress and reactive oxygen species (ROS) may be important factors leading to liver fibrosis. NADPH oxidase 4 (NOX4) is the main source of ROS in hepatic fibrosis, but the mechanism by which NOX4 regulates oxidative stress is not fully understood. β-Arrestin2 is a multifunctional scaffold protein that regulates receptor endocytosis, signaling and trafficking. In this study, we investigated whether β-arrestin2 regulated oxidative stress in hepatic fibrosis. Both β-arrestin2 knockout (*Arrb*2 KO) mice and wild-type mice were intraperitoneally injected with carbon tetrachloride ($CCl_4$) to induce hepatic fibrosis. *Arrb*2 KO mice showed significantly attenuated liver fibrosis, decreased ROS levels and NOX4 expression, and reduced collagen levels in their livers. In vitro, NOX4 knockdown significantly inhibited ROS production, and decreased expression of alpha-smooth muscle actin in angiotensin II-stimulated human HSC cell line LX-2. Through overexpression or depletion of β-arrestin2 in LX-2 cells, we revealed that decreased β-arrestin2 inhibited ROS levels and NOX4 expression, and reduced collagen production; it also inhibited activation of ERK and JNK signaling pathways. These results demonstrate that β-arrestin2 deficiency protects against liver fibrosis by downregulating ROS production through NOX4. This effect appears to be mediated by ERK and JNK signaling pathways. Thus, targeted inhibition of β-arrestin2 might reduce oxidative stress and inhibit the progression of liver fibrosis.

**Keywords:** liver fibrosis; hepatic stellate cells; β-arrestin2; oxidative stress; NOX4; ROS; α-SMA; U0126; SP600125

*Acta Pharmacologica Sinica* (2021) 42:1090–1100; https://doi.org/10.1038/s41401-020-00545-9

## INTRODUCTION

Hepatic fibrosis occurs due to excessive deposition of extracellular matrix (ECM) after repeated or continuous stimulation of pathogenic factors [1]. Although early stage liver fibrosis is considered to be a reversible pathological process, it can progress to cirrhosis and even liver cancer, resulting in increased morbidity and mortality, if not managed [2]. Hepatic stellate cells (HSCs) play a significant role in the development of hepatic fibrosis. They are activated and transformed into myofibroblasts when damaged by pathogenic factors and participate in the injury repair process [3].

Oxidative stress has been identified as a potential mechanism of fibrotic diseases. Oxidative stress occurs due to an imbalance between antioxidant capacity and reactive oxygen species (ROS) production by specific enzymes [4]. Oxidative stress and ROS production are likely significant mechanisms underlying HSCs activation and liver injury [5]. ROS production may be driven by multicomponent nicotinamide adenine dinucleotide phosphate (NADPH) oxidase (NOX) family enzyme complexes [6]. Of the seven mammalian NOX subtypes (NOX1, NOX2, NOX3, NADPH oxidase 4 (NOX4), NOX5, and DUOX1–2) [7], NOX1, NOX2, and NOX4 are expressed in the liver [8]. Mounting evidence indicates that NOX4 expression is high in HSCs and hepatocytes. NOX4 is an important source of ROS production during signal transduction [9], and its role in hepatic fibrosis has attracted increasing attention; however, the mechanism through which NOX4-mediated ROS production is regulated in hepatic fibrosis has not been thoroughly studied.

β-Arrestin2 is a multifunctional regulatory protein that acts as an adapter and scaffold protein for G-protein-coupled receptors (GPCRs) and contributes to desensitization and receptor internalization [10]. More recently, β-arrestin2 was shown to be an important signaling scaffold that facilitates the activation of numerous effector pathways, such as the mitogen-activated protein kinase (MAPK) pathway [11]. Our previous studies showed that the expression of β-arrestin2 in liver tissues gradually increases with the progression of porcine serum-induced hepatic fibrosis [12] and that β-arrestin2 depletion may exert protective effects on acute liver injury in mice [13]. However, it is unclear whether β-arrestin2 plays a role in regulating oxidative stress in chronic liver fibrosis.

In the current study, we employed β-arrestin2 knockout (*Arrb2* KO) mice to elucidate the function of β-arrestin2 in regulating oxidative stress in chronic hepatic fibrosis. We hypothesize that β-arrestin2 may regulate ROS production via NOX4 and is essential for the progression of liver fibrosis.

[1]Institute of Clinical Pharmacology, Anhui Medical University, Key Laboratory of Anti-inflammatory and Immune Medicine, Ministry of Education, Anhui Collaborative Innovation Center of Anti-inflammatory and Immune Medicine, Hefei 230032, China
Correspondence: Wu-yi Sun (sunwuyi51@aliyun.com) or Wei Wei (wwei@ahmu.edu.cn)
These authors contributed equally: Jia-jia Du, Jia-chang Sun, Nan Li

Received: 24 April 2020 Accepted: 21 September 2020
Published online: 28 October 2020

## MATERIALS AND METHODS

### Animals and treatments

*Arrb2* KO mice on the C57BL/6 background were obtained from Jackson Laboratory (Maine, USA). All mice were genotyped 14 days after birth. DNA samples were prepared from tail tips using a tissue PCR kit from Kapa Biosystems (Massachusetts, USA) and subjected to triplex PCR as previously described [14]. We employed *Arrb2* KO mice aged 6–8 weeks and age- and sex-matched wild-type (WT) C57BL/6J mice for all experiments. All animals were housed under specific-pathogen-free (SPF) conditions at 25 ± 2 °C with a relative humidity of 55% ± 10% and a 12 h light/dark cycle. All experiments were approved by the Ethics Review Committee for Animal Experimentation at the Institute of Clinical Pharmacology, Anhui Medical University.

*Arrb2* KO mice and WT mice were randomly assigned to the carbon tetrachloride ($CCl_4$)-induced hepatic fibrosis group or the vehicle control group ($n = 6$ in each group). Mice in the model group were intraperitoneally injected with 5 mL/kg 10% $CCl_4$ (Shanghai Lingfeng Chemical Factory, Shanghai, China) dissolved in corn oil two times per week. Vehicle control mice received an equivalent volume of corn oil. The mice were euthanized 2, 4, or 8 weeks after $CCl_4$ injection. A portion of the liver of each mouse was preserved in 10% formaldehyde for histological analyses, and another portion of each liver was immediately frozen in liquid nitrogen and quickly stored in a refrigerator at −80 °C for subsequent analysis.

### Cell culture and treatment

The immortalized human HSC cell line LX-2 was obtained from the Cell Bank of the Chinese Academy of Sciences (Shanghai, China). The cells were routinely grown in Dulbecco's modified Eagle's medium (DMEM) (Gibco, CA, USA) containing 10% fetal bovine serum (Zhejiang Tianhang Biotechnology Co., Ltd, Zhejiang, China) and 1% penicillin-streptomycin solution (Beyotime Biotechnology, Shanghai, China). The cells were incubated at 37 °C in a humidified chamber with 5% $CO_2$. The literature indicates that angiotensin II (AngII) treatment significantly elevates ROS production in HSCs [15]. Thus, we chose AngII (MedChemExpress, NJ, USA) to induce ROS production in vitro. LX-2 cells were used to confirm the potential role of β-arrestin2 in AngII-induced oxidative stress associated with fibrosis development, i.e., ROS production.

### Histopathological analysis

Mouse liver samples were excised, fixed in 10% formalin for 24 h, embedded in paraffin, and serially sectioned at a thickness of 5 μm. Pathological changes in liver tissues were observed by hematoxylin and eosin staining (H&E). Briefly, prepared liver slices were stained with hematoxylin for 5 min followed by eosin for 3 min. Changes in nuclei and cytoplasm were observed in H&E-stained sections. To assess collagen deposition, other sections were subjected to Masson trichrome staining. Briefly, liver sections were stained at 25 °C with acid ponceau/solferino for 1 min followed by aniline blue for 5 min. Cell nuclei were stained with hematoxylin for 6 min. In the Masson trichrome-stained tissues, the blue areas indicated areas of collagen deposition. Histological changes in the liver were viewed under an Olympus BX53 microscope (Olympus Corporation, Tokyo, Japan).

### In situ detection of ROS levels

Fresh liver tissues were embedded in optimum cutting temperature compound (Sakura, CA, USA), frozen in liquid nitrogen immediately after harvest, and stored at −80 °C until they were sliced. Liver tissue sections (10-μm thick) were prepared with a Leica CM1950 cryostat (Leica Microsystems GmbH, Nussloch, Germany). The liver sections were covered with 5 μmol/L dihydroethidium (DHE) (Beyotime Biotechnology) dissolved in dimethyl sulfoxide and placed in the dark at 37 °C for 30 min. After this staining procedure, the sections were rinsed with phosphate-buffered saline (PBS) and sealed with coverslips. Photographs of the sections were obtained using an Olympus IX-71 fluorescence microscope (Olympus Corporation). ImageJ software (National Institutes of Health, MD, USA) was used to quantify staining intensities and compute the averages.

### Immunostaining and confocal microscopy

To prevent nonspecific staining, all sections were first immersed in 3% BSA for 2 h at room temperature and then rinsed three times with PBS for 3 min. The sections were then incubated with a monoclonal primary antibody against β-arrestin2 (Santa Cruz Biotechnology, CA, USA) and a monoclonal primary antibody against NOX4 (Abcam Biotechnology, Cambridge, UK) for 12 h at 4 °C in the dark. Negative control sections were incubated with PBS instead of primary antibody. The sections were then washed three times with PBS, probed with Alexa Fluor 488-conjugated and Alexa Fluor 555-conjugated secondary antibodies (Thermo Fisher, MA, USA), and counterstained with 4′,6-diamidino-2-phenylindole (DAPI) (Beyotime Biotechnology) to visualize the nuclei. Finally, the expression of β-arrestin2 and NOX4 was assessed with a Leica TCS SP8 laser scanning confocal microscope (Leica Biosystems, Wetzlar, Germany).

### Silencing of β-arrestin2 and NOX4 gene expression with small interfering RNAs (siRNAs)

siRNA oligonucleotides targeting NOX4 and β-arrestin2 were designed and synthesized by Shanghai GenePharma (Shanghai, China). A scrambled RNA duplex was used as a negative control. The sequences were as follows: NOX4 siRNA, sense 5'-CCAUGUGCCGAACACUCUUTT-3' and antisense 5'-AAGAGUGUUCGGCACAUGGTT-3'; β-arrestin2 siRNA, sense 5'-CCAACCUCAUUGAAUUUGATT-3' and antisense 5'-UCAAAUUCAAUGAGGUUGGTT-3'. LX-2 cells were seeded in 6-well plates 24 h before transfection. GP-siRNA-Mate Plus (GenePharma) transfection reagent was shaken well, and equal volumes of RNA oligo and transfection reagent were mixed and incubated for 10–15 min before being applied to cells for transfection. The LX-2 cells were incubated for 48 h after transfection, and protein was then extracted for Western blotting analysis.

### DNA transfection

To overexpress β-arrestin2 in this study, we used a pcDNA3 expression plasmid encoding β-arrestin2. U0126 (an ERK1/2 inhibitor) and SP600125 (a JNK inhibitor) were obtained from MedChemExpress. LX-2 cells were seeded in six-well plates in the presence or absence of 10 μmol/L U0126 or SP600125. Then, the cells were transiently transfected with the above β-arrestin2 overexpression vector using Lipofectamine 3000 (Invitrogen Life Technologies, CA, USA) according to the manufacturer's recommendations.

### Western blot analysis

In general, protein was isolated from liver tissues or LX-2 cells in RIPA protein lysis buffer containing 1 mmol/L phenylmethylsulfonyl fluoride for 30 min at 4 °C. Particulates were removed by centrifugation for 30 min at 14,000 × *g*, and protein levels were determined using a bicinchoninic acid protein quantitation kit (Thermo Fisher). The proteins were resolved by sodium dodecyl sulfate–polyacrylamide gel electrophoresis, after which they were transferred onto polyvinylidene fluoride membranes (Millipore, MA, USA). The membranes were blocked with 5% dried skimmed milk in 0.05% Tween 20-PBS for 2 h and incubated with primary antibodies overnight at 4 °C. Antibodies against β-arrestin2, alpha-smooth muscle actin (α-SMA), collagen I, collagen III, tissue inhibitor of metalloprotease protein 1 (TIMP-1), and matrix metalloproteinase 13 (MMP-13) were obtained from Santa Cruz Biotechnology. Antibodies against phospho-ERK (p-ERK), ERK, phospho-JNK (p-JNK), and JNK were purchased from Cell Signaling

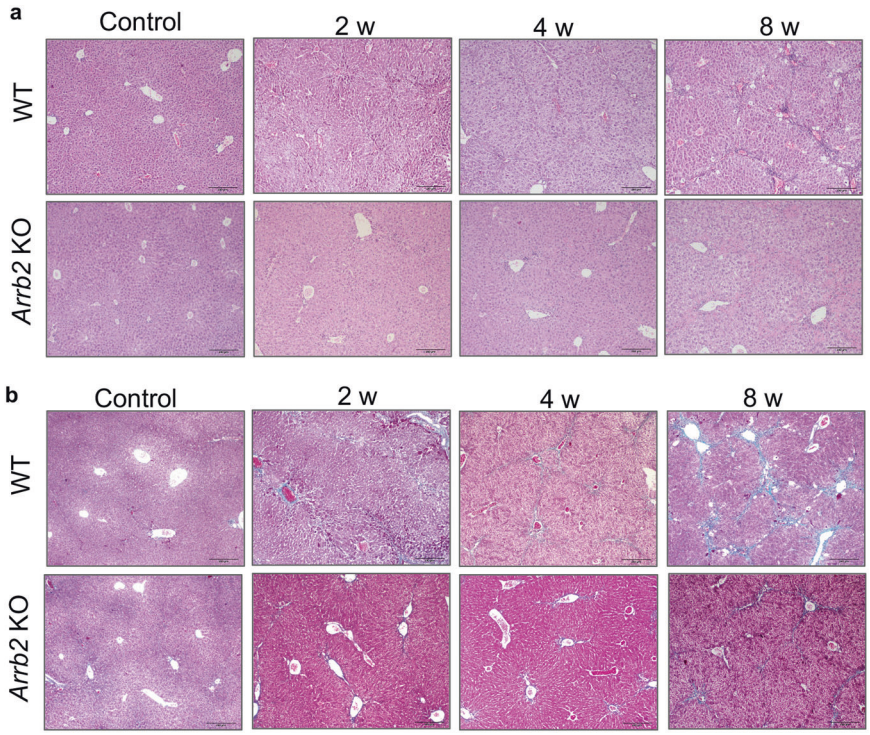


**Fig. 1 β-Arrestin2 deficiency alleviates carbon tetrachloride ($CCl_4$)-induced liver fibrosis in mice. a** Representative images of hematoxylin and eosin (H&E) staining of the livers of β-arrestin2 knockout (*Arrb2* KO) and wild-type (WT) mice (×100 magnification). **b** Liver sections from *Arrb2* KO and WT mice were subjected to Masson trichrome staining. Representative images are shown (×100 magnification).

Technology (MA, USA). A primary antibody against NOX4 was purchased from Abcam Biotechnology. The membranes were treated with secondary antibodies on the 2nd day and incubated for 2 h. The proteins were quantitated with the ImageQuant LAS 4000mini imaging system (GE Healthcare Bio-Sciences AB, Uppsala, Sweden). Protein expression levels were defined as gray values, which were determined with ImageJ software. β-Actin expression was used as an internal control.

### Determination of intracellular ROS levels

2′,7′-Dichlorodihydrofluorescein diacetate (DCFH-DA) is a cell permeable lipophilic compound incorporating DCFH, which can be oxidized to 2′,7′-dichlorofluorescein (DCF) under conditions of oxidative stress [16]. The level of DCF fluorescence indicates the levels of intracellular ROS. LX-2 cells were seeded in six-well plates. After treatment, the LX-2 cells were incubated with DCFH-DA (Beyotime Biotechnology) for 20 min at 37 °C and were then washed three times with culture medium. The fluorescence intensity of treated cells was measured using a fluorescence microscope [17]. Images were acquired by using an Olympus IX-71 microscope. Cellular fluorescence intensity was also detected using a CytoFLEX flow cytometer (Beckman, CA, USA). Cell pellets collected after washing were homogenized with 1 mL of PBS buffer and analyzed by flow cytometry at excitation and emission wavelengths of 488 and 525 nm, respectively. Intracellular ROS levels were calculated based on the DCF fluorescence intensity.

### Statistical analysis

All results are expressed as the means ± SD. Each experiment was conducted at least three times. The statistical significance of differences between multiple groups was assessed using one-way analysis of variance. For all analytical studies, $P < 0.05$ was considered significant.

## RESULTS

### β-Arrestin2 deficiency attenuates $CCl_4$-induced liver fibrosis

To investigate the function of β-arrestin2 in the development of liver fibrosis, we established a $CCl_4$-induced liver fibrosis model in β-arrestin2-deficient mice. H&E and Masson stainings were employed to observe the degree of hepatic damage. The results of H&E staining are shown in Fig. 1a. In control mice, H&E staining showed normal lobular architecture. At 4 weeks post $CCl_4$ injection, increased infiltration of inflammatory cells and hepatocyte ballooning were observed. At 8 weeks after $CCl_4$ injection, increased lobular inflammation, necrosis, and marked fatty degeneration were detected in the $CCl_4$-injured livers of WT mice. β-Arrestin2-deficient mice exhibited less infiltration of inflammatory cells and hepatic steatosis and necrosis than WT mice. Since collagen is a marker of fibrosis, collagen deposition was detected by Masson staining. In normal livers, small quantities of collagen were observed, mainly in the portal area and central vascular walls. At 4 weeks after $CCl_4$ injection, the portal area and central vascular wall showed small accumulations of blue stain, while extensive collagen deposition and pseudolobular formations were seen at 8 weeks post $CCl_4$ injection. *Arrb2* KO mice showed significantly less interstitial and perivascular fibrosis than WT mice (Fig. 1b). These data preliminarily suggest that β-arrestin2 knockout attenuates hepatic fibrosis.

### β-Arrestin2 deficiency reduces ROS production in the livers of fibrotic mice

To determine whether β-arrestin2 plays a role in ROS production, we used the fluorescent probe DHE to observe changes in ROS levels [18]. DHE can be oxidized to ethidium, resulting in the amplification of red fluorescence and punctate nuclear staining that indicates ROS production [19]. As shown in Fig. 2, ROS production was significantly increased in the livers of $CCl_4$-injected mice compared with those of normal mice at 8 weeks. In contrast,

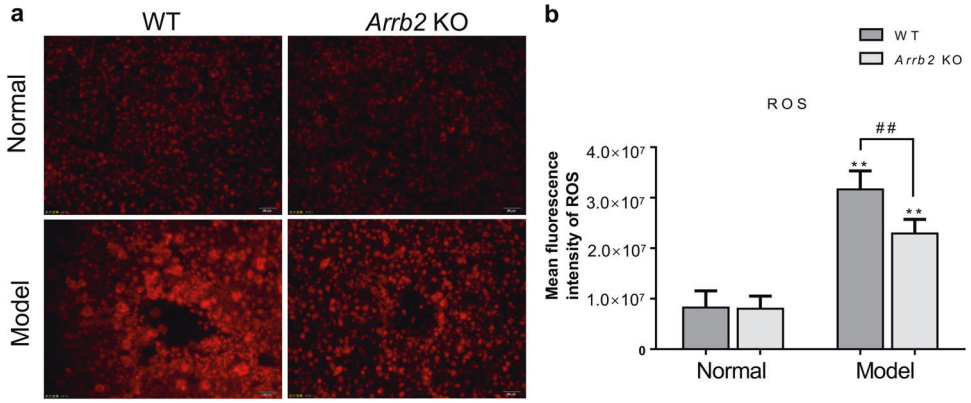


**Fig. 2 β-Arrestin2 deficiency reduces reactive oxygen species (ROS) production in the livers of fibrotic mice.** ROS generation in fresh livers was detected using dihydroethidium (DHE) staining. **a** Representative micrographs of liver sections stained with DHE. Bright red spots indicate ROS production (×400 magnification). **b** ROS production was quantitated by measuring the fluorescence intensity ($n = 8$ images of liver sections from four mice per group). $^{**}P < 0.01$ compared with the normal group; $^{\#\#}P < 0.01$ compared with the WT model group.

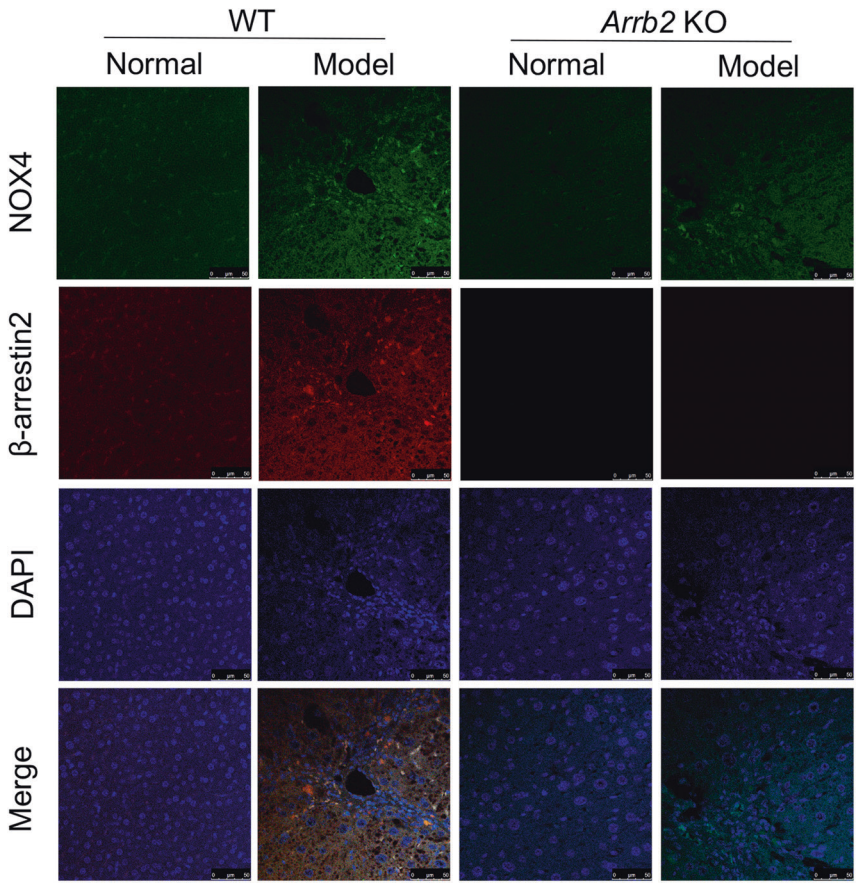


**Fig. 3 Expression of NADPH oxidase 4 (NOX4) is downregulated in the liver tissues of β-arrestin2-deficient mice.** Liver sections were subjected to double immunofluorescence staining with antibodies against NOX4 (green) and β-arrestin2 (red). DAPI was used to counterstain the nuclei (blue). Representative pictures of liver sections were examined by immunofluorescence confocal microscopy (×400 magnification).

the production of ROS in *Arrb2* KO mice was dramatically lower than that in WT mice. Collectively, these results indicate that ROS levels may be regulated by β-arrestin2. Absence of β-arrestin2 may be able to downregulate ROS production in liver fibrosis.

NOX4 expression is downregulated in liver tissues of β-arrestin2-deficient mice

Since NOX4 is the major source of ROS, we used double immunofluorescence staining to detect the expression of NOX4 and β-arrestin2 in the liver tissues of normal and $CCl_4$-induced fibrotic mice (8 weeks post $CCl_4$ injection). Single channel scanning displayed β-arrestin2 and NOX4 positive signals as red and green fluorescent foci, respectively. Overlapping distribution was visualized as yellow. As shown in Fig. 3, the fluorescence intensity of β-arrestin2 and NOX4 was enhanced in WT fibrotic mice compared to control WT mice. The immunofluorescence staining intensity of both β-arrestin2 and NOX4 was reduced in *Arrb2* KO mice compared with WT mice. Western blotting further

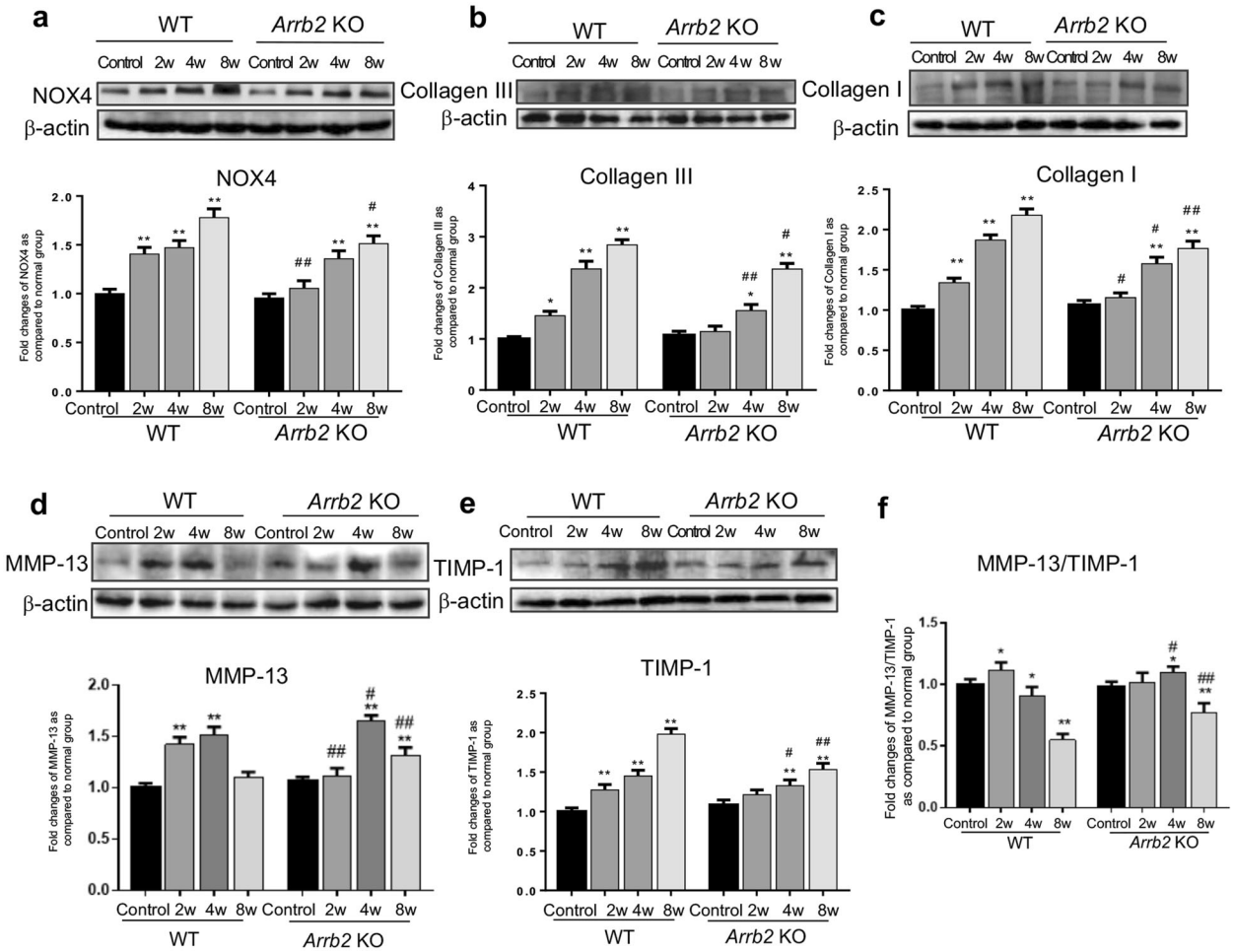


**Fig. 4 Western blot analysis of NOX4 and extracellular matrix (ECM)-related proteins expression in liver tissues of hepatic fibrosis mice.** Liver homogenates were subjected to immunoblotting for NOX4, collagen III, collagen I, matrix metalloproteinase (MMP)-13, and tissue inhibitor of metalloprotease protein (TIMP)-1. Representative pictures of bands for NOX4 (**a**), collagen III (**b**), collagen I (**c**), MMP-13 (**d**), and TIMP-1 (**e**) are shown. **f** The ratio of MMP-13/TIMP-1 ($n = 5$ for each group). Densitometry values in the histograms are expressed as the fold change relative to the value of the WT normal group, which was assigned a value of 1. $^{*}P < 0.05$, $^{**}P < 0.01$ compared with the normal group; $^{\#}P < 0.05$, $^{\#\#}P < 0.01$ compared with the WT model group at the same time point.

confirmed that NOX4 expression was reduced upon β-arrestin2 knockout (Fig. 4a). These data demonstrate that β-arrestin2 deficiency may decrease ROS production in a NOX4-mediated manner.

β-Arrestin2 knockout reduces collagen deposition and maintains the MMP-13/TIMP-1 balance in fibrotic mice

$CCl_4$-induced liver fibrosis is associated with a marked upregulation of collagen I and collagen III expression [20]. As shown in Fig. 4b, c, the expression of collagen I and collagen III incrementally increased in the livers of WT fibrosis mice compared to those of control WT mice, and *Arrb*2 KO mice exhibited a decrease in collagen I and III expression compared with WT mice. TIMP-1 is an endogenous inhibitor of MMP-mediated ECM degradation. It has been suggested that upregulation of TIMP-1 expression participates in the development of hepatic fibrosis [21]. MMP-13 plays an essential role in the degradation of components of the ECM, including collagen types I and III [22]. To investigate the role of β-arrestin2 deficiency in ECM degradation in $CCl_4$-induced hepatic fibrosis, we detected the protein expression of TIMP-1 and MMP-13 in liver tissues. Our data suggest that MMP-13 expression was increased in *Arrb2* KO mice compared with WT mice at 4 and 8 weeks after $CCl_4$ injection (Fig. 4d). TIMP-1 expression was obviously increased in the fibrotic livers of WT mice compared to the livers of control WT mice, while β-arrestin2 deficiency significantly inhibited TIMP-1 expression (Fig. 4e). A previous study showed that the balance between MMPs and TIMPs regulates ECM turnover and remodeling [23]. Thus, it was essential to examine the MMP/TIMP ratio. We found that the ratio of MMP-13 to TIMP-1 was significantly increased in *Arrb2* KO mice compared with WT mice (Fig. 4f). The above results indicate that *Arrb*2 KO decreases NOX4 expression and ROS levels in vivo and reduces ECM deposition in liver fibrosis.

Downregulation of NOX4 in HSCs contributes to decreased ROS and collagen levels

Considering that AngII treatment significantly elevates ROS production in HSCs [15], AngII-stimulated human HSCs (LX-2 cells) were used as a cellular model of ROS production in vitro. As α-SMA is a marker of activated HSCs, we examined the expression of α-SMA in HSCs. LX-2 cells were synchronized with serum-free DMEM and stimulated with AngII ($10^{-8}$, $10^{-7}$, $10^{-6}$, or $10^{-5}$ mol/L) for 24 h. As shown in Fig. 5a, NOX4, α-SMA and β-arrestin2 expression was increased in cells stimulated with $10^{-6}$–$10^{-5}$ mol/L AngII compared with unstimulated cells. Therefore, $10^{-6}$ mol/L AngII was used as a stimulant in the subsequent experiment.

To further investigate the role of NOX4 in β-arrestin2 deficiency-mediated ROS inhibition and collagen suppression, we next used

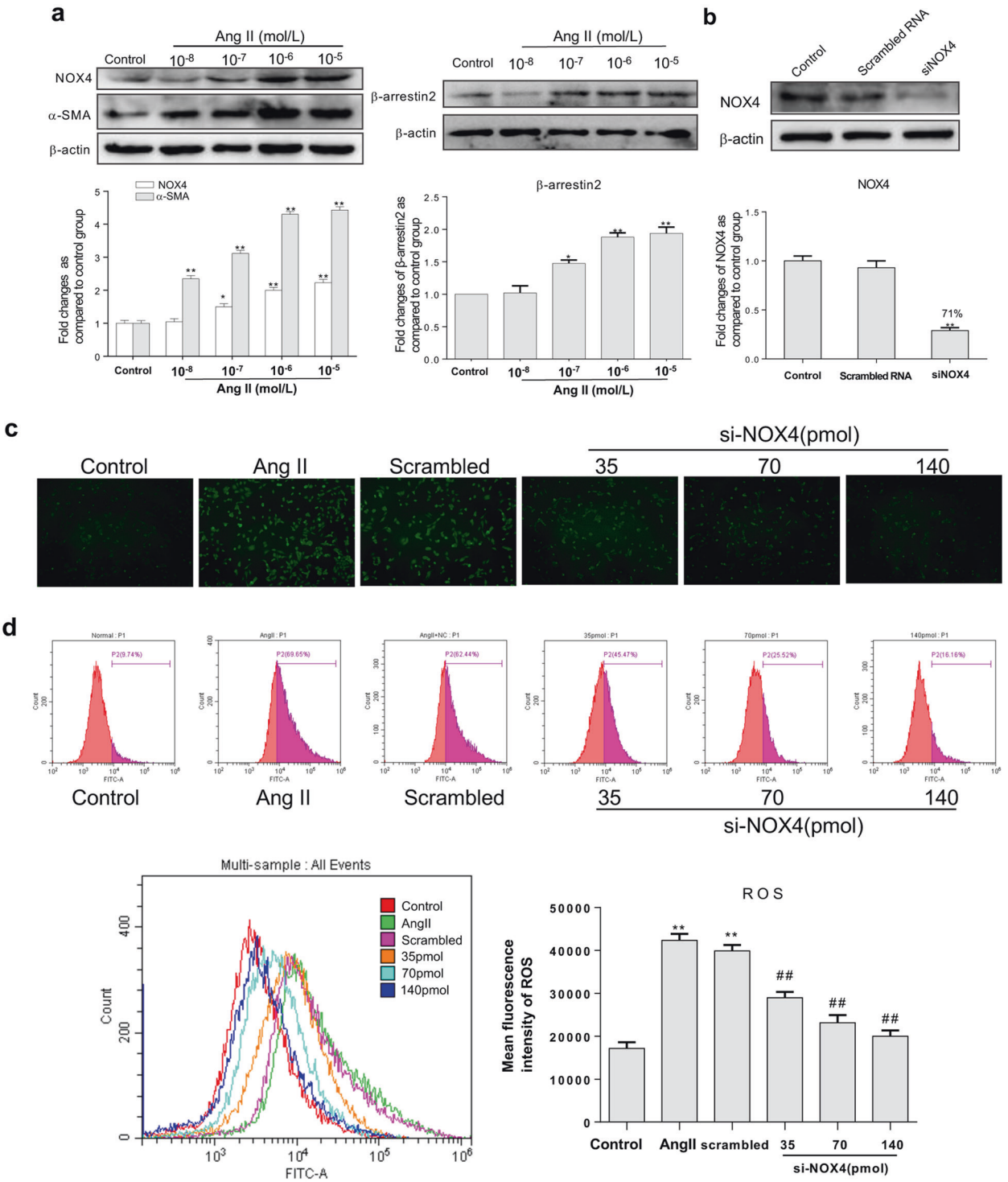


**Fig. 5 Downregulation of NOX4 in HSCs contributes to inhibition of ROS production. a** NOX4, α-SMA, and β-arrestin2 expression in LX-2 cells stimulated with AngII ($10^{-8}$, $10^{-7}$, $10^{-6}$, or $10^{-5}$ mol/L). LX-2 cells not stimulated with AngII were used as baseline controls. **b** Protein level of NOX4 in LX-2 cells transfected with siRNA targeting NOX4. **c** ROS levels were measured with the 2′,7′-dichlorodihydrofluorescein diacetate (DCFH-DA) fluorescent probe. Fluorescent photographs show the effect of NOX4 siRNA on ROS production in LX-2 cells stimulated by AngII. **d** Decreased ROS levels were observed in NOX4 siRNA-transfected LX-2 cells, as detected by flow cytometry ($n = 5$ per group). $^{*}P < 0.05$, $^{**}P < 0.01$ compared with the control group; $^{\#\#}P < 0.01$ compared with the scrambled siRNA group.

an siRNA targeting NOX4 to silence the expression of NOX4 in HSCs stimulated with AngII. Transfection of NOX4 siRNA into LX-2 cells significantly decreased NOX4 protein expression (Fig. 5b). As expected, the results of fluorescence microscopy (Fig. 5c) and flow cytometry (Fig. 5d) showed that the DCH fluorescence intensity in AngII-stimulated LX-2 cells was significantly higher than that in LX-2 cells not stimulated with AngII, indicating that AngII stimulated ROS formation. Meanwhile, ROS production in HSCs was significantly inhibited after transfection with NOX4 siRNA. Further experiments showed that when NOX4 expression was inhibited by

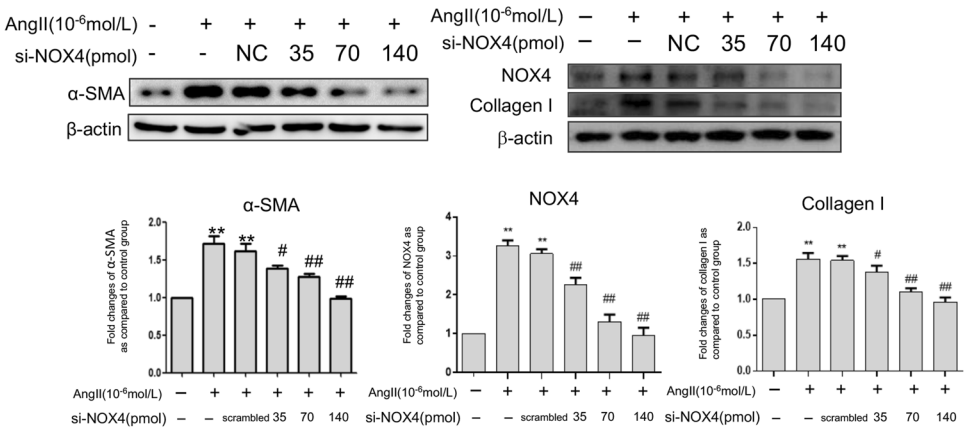


**Fig. 6 NOX4 siRNA reduces the expression of collagen in LX-2 cells stimulated by AngII.** Western blotting indicated that si-NOX4 treatment decreased α-SMA and collagen I protein expression in a concentration-dependent manner. Densitometry values in the histograms are expressed as the fold change relative to the value of the control group, which was assigned a value of 1. The data are presented as the mean ± SD of at least four independent experiments. $^{**}P < 0.01$ compared with the control group; $^{\#}P < 0.05$, $^{\#\#}P < 0.01$ compared with the scrambled siRNA group.

NOX4 siRNA, α-SMA expression and collagen I levels were decreased compared with those in AngII-treated untransfected cells (Fig. 6). The above results indicate that NOX4 silencing in HSCs significantly inhibits ROS production and thus decreases α-SMA and collagen levels.

β-Arrestin2 regulates ROS production by modulating NOX4 in vitro

ROS production was decreased during liver fibrosis in *Arrb2* KO mice, while the role of β-arrestin2 in this process still remains poorly understood. Thus, we focused on the potential role of β-arrestin2 in ROS production by HSCs in vitro. We first transfected a plasmid encoding β-arrestin2 into LX-2 cells. Western blotting confirmed that β-arrestin2 was successfully overexpressed and that overexpression of β-arrestin2 increased NOX4 and α-SMA levels in LX-2 cells (Fig. 7a). Furthermore, the production of ROS in LX-2 cells was significantly increased when β-arrestin2 was overexpressed (Fig. 7b). Because we found that overexpression of β-arrestin2 is closely associated with increased NOX4 expression and ROS levels in HSCs, we hypothesized that loss of β-arrestin2 in HSCs inhibits ROS production. To that end, we transfected β-arrestin2 siRNA into LX-2 cells. The expression of β-arrestin2 was significantly decreased in cells transfected with β-arrestin2 siRNA compared to untransfected cells, as demonstrated by Western blotting (Fig. 7c). Further experiments showed that when β-arrestin2 expression was reduced by β-arrestin2 siRNA, the ROS fluorescence intensity was significantly decreased in LX-2 cells stimulated with AngII (Fig. 7d). Meanwhile, transfection with β-arrestin2 siRNA significantly inhibited the AngII-induced increase in α-SMA and collagen I expression. To further determine the mechanism by which β-arrestin2 knockdown reduces oxidative stress, NOX4 expression was quantitated. NOX4 expression was significantly decreased in cells with β-arrestin2 knockdown compared to scrambled siRNA control cells (Fig. 7e). The above data indicate that β-arrestin2 knockdown inhibits ROS production, which correlates with a decrease in NOX4 expression, and support the in vivo studies showing that β-arrestin2 deficiency is associated with reduced ROS production.

β-Arrestin2 regulates oxidative stress via the ERK and JNK signaling pathways

β-Arrestin2, as a signal regulatory protein, has been demonstrated to activate signaling cascades independent of G-protein activation, including the MAPK and phosphatidylinositol-3 kinase pathways [24]. Previous studies have indicated that the ERK and JNK signaling pathways are involved in the pathological process of fibrosis [25, 26]. However, whether β-arrestin2 regulates oxidative stress through JNK or ERK signaling in hepatic fibrosis has not been elucidated to date. Western blotting was used to detect the effect of β-arrestin2 overexpression on the activation of the ERK and JNK pathways. The results showed that overexpression of β-arrestin2 promoted the activation of the ERK and JNK pathways (Fig. 8a). To investigate whether β-arrestin2 regulates oxidative stress through these signaling pathways, we transfected HSCs with an expression vector carrying β-arrestin2 in the presence or absence of an ERK inhibitor (U0126) or a JNK inhibitor (SP600125). Inhibition of ERK or JNK effectively blocked the upregulation of NOX4 and ROS in β-arrestin2-overexpressing LX-2 cells compared with cells that were transfected with the β-arrestin2 plasmid only (Figs. 7b and 8b). Our results suggest that β-arrestin2 expression in HSCs may be through increasing ERK and JNK activation, leading to upregulation of NOX4 expression and ROS production. We next examined the effect of siRNA targeting β-arrestin2 on the activation of ERK and JNK in HSCs stimulated with AngII. As shown in Fig. 8c, d, activation of ERK and JNK in AngII-stimulated cells was significantly increased compared with that in unstimulated cells, while p-ERK and p-JNK expression was decreased in cells that were treated with β-arrestin2 siRNA and AngII. Combined with the previously mentioned finding that β-arrestin2 siRNA decreases NOX4 expression and ROS levels in LX-2 cells, these results indicate that interfering with the expression of β-arrestin2 downregulates NOX4 and ROS levels may be through the ERK and JNK pathways.

## DISCUSSION

Hepatic fibrosis is a pathological condition characterized by long-term stimulation of pathogenic factors. Hepatocyte damage accompanied by inflammation and innate immune system activation results in fibrosis through activation of HSCs and deposition of ECM proteins, including collagen types I and III [27, 28]. Liver fibrosis is a vital and reversible process of wound healing, but the mechanisms underlying liver fibrosis have not been fully elucidated. There is mounting evidence that abnormal β-arrestin2 expression is involved in different types of fibrotic diseases [29], such as lung [30], renal [31], and cardiac fibrosis [32]. Our previous studies suggested that porcine serum-induced hepatic fibrosis progression correlates with gradually increasing expression of β-arrestin2 in hepatic tissues [12]. In the present study, we established a liver fibrosis model by intraperitoneally injecting $CCl_4$ into *Arrb2* KO mice. H&E and Masson staining results

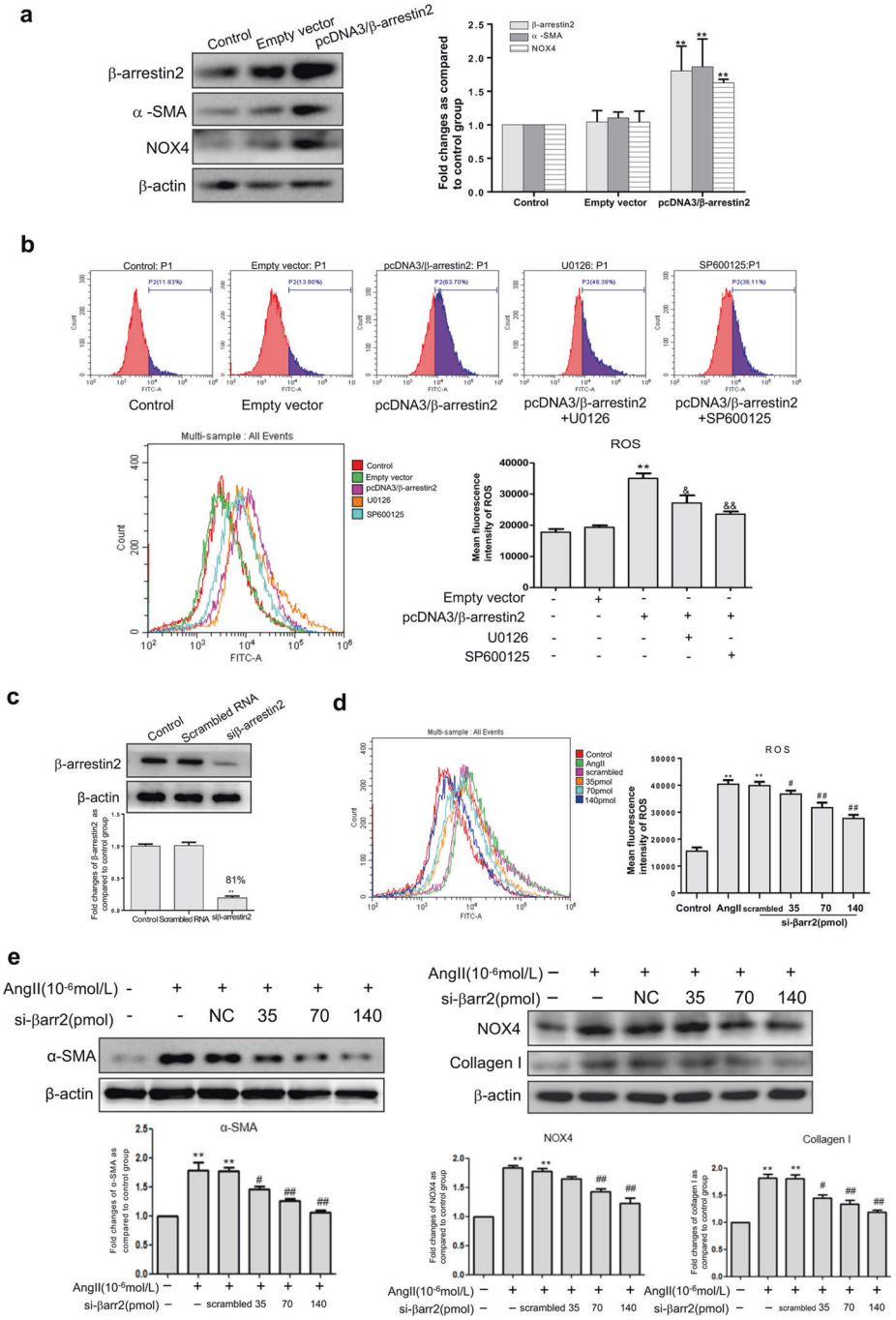


**Fig. 7 β-Arrestin2 regulates ROS production by modulating NOX4. a** β-Arrestin2 was overexpressed by transfecting a pcDNA3 expression plasmid encoding β-arrestin2 into LX-2 cells, and overexpression of β-arrestin2 significantly promoted α-SMA and NOX4 expression in LX-2 cells. **b** ROS levels in β-arrestin2-overexpressing LX-2 cells in the presence or absence of ERK inhibitor (U0126) or JNK inhibitor (SP600125) were measured by flow cytometry. Overexpression of β-arrestin2 significantly increased ROS production, while pretreatment with U0126 or SP600125 in LX-2 cells obviously blocked ROS production. $^{**}P < 0.01$ compared with the empty vector group; $^{\&}P < 0.05$, $^{\&\&}P < 0.01$ compared with the β-arrestin2 overexpression group. **c** The protein level of β-arrestin2 was significantly decreased in LX-2 cells transfected with β-arrestin2 siRNA. **d** Intracellular ROS levels in LX-2 cells were measured by flow cytometry with the DCFH-DA probe after interfering with β-arrestin2. The histogram shows that when β-arrestin2 expression was reduced by β-arrestin2 siRNA, ROS fluorescence intensity was significantly decreased in LX-2 cells stimulated with AngII. **e** Representative immunoblots show the effects of β-arrestin2 knockdown on the expression of α-SMA, NOX4, and collagen I in LX-2 cells upon AngII treatment. Downregulation of β-arrestin2 resulted in the decreased expression of α-SMA, NOX4, and collagen I proteins. The data are presented as the mean ± SD of at least four independent experiments. $^{**}P < 0.01$ compared with the control group; $^{\#}P < 0.05$, $^{\#\#}P < 0.01$ compared with the scrambled siRNA group.

showed gradual progression of fibrosis in $CCl_4$-injured WT mice. *Arrb2* KO mice showed less inflammation and collagen deposition than WT mice, which suggests that β-arrestin2 deficiency might alleviate liver fibrosis. Furthermore, Western blotting indicated that the expression of collagen type I and type III was lower in the liver tissues of *Arrb2* KO mice than in those of WT mice. ECM synthesis and degradation are mainly regulated by MMPs and TIMPs. MMPs can promote ECM degradation, while TIMPs can

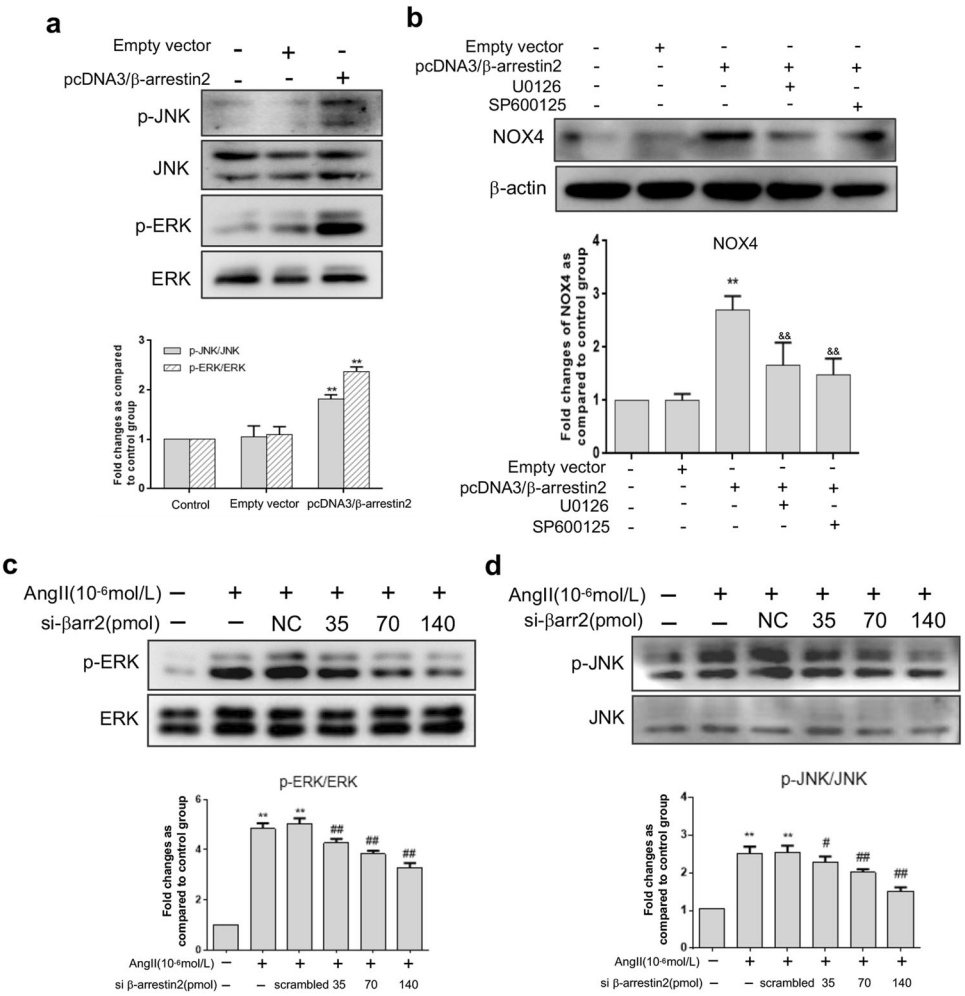


**Fig. 8 β-Arrestin2 regulates oxidative stress via the ERK and JNK signaling pathways. a** Overexpression of β-arrestin2 significantly promoted the activation of the ERK and JNK signaling pathways in LX-2 cells. **b** Effects of transfecting β-arrestin2 overexpression plasmid on NOX4 expression in LX-2 cells pretreated with an ERK inhibitor (U0126) or JNK inhibitor (SP600125). Inhibition of ERK or JNK effectively blocked the upregulation of NOX4 in β-arrestin2-overexpressing LX-2 cells. $^{**}P < 0.01$ compared with the empty vector group; $^{\&\&}P < 0.01$ compared with the β-arrestin2 overexpression group. Representative immunoblots show the expression of p-ERK (**c**) and p-JNK (**d**) in AngII-stimulated LX-2 cells after β-arrestin2 knockdown. Decreased expression of p-ERK and p-JNK in LX-2 cells was observed after transfection with β-arrestin2 siRNA. The data are presented as the mean ± SD of at least four independent experiments. $^{**}P < 0.01$ compared with the control group; $^{\#}P < 0.05$, $^{\#\#}P < 0.01$ compared with the scrambled siRNA group.

repress ECM degradation by inhibiting MMP activity [33]. MMP-13 is the main interstitial collagenase in rodents. TIMP-1 is widely expressed in body tissues and can inhibit most MMPs [34]. Therefore, we chose to study the ratio of MMP-13/TIMP-1 in vivo to explore the balance between MMP/TIMP-mediated fiber ablation. Our results showed that β-arrestin2 knockout promoted fiber degradation by affecting the balance between MMP-13 and TIMP-1, thereby countering persistent hepatic fibrosis. Our present study suggests that β-arrestin2 depletion can decrease collagen deposition and alleviate liver fibrosis.

Oxidative stress is a condition in which an organism or cells produce excessive ROS, which then damage lipids, proteins, and DNA [35]. Cumulative studies in mice and humans have shown that oxidative stress is inseparably related to the pathogenesis of hepatic fibrosis [36]. ROS can promote the progression of hepatic fibrosis by directly activating HSCs. Activated HSCs then increase the production of ROS [37]. In our present study, staining of frozen liver sections with the fluorescent probe DHE indicated a significant increase in ROS levels in fibrotic WT mice compared to control WT mice. Liver ROS levels in *Arrb2* KO mice were significantly lower than those in WT mice. In vitro studies showed that ROS production was obviously decreased in HSCs transfected with β-arrestin2 siRNA, as detected by flow cytometry. In contrast, ROS production was increased in HSCs overexpressing β-arrestin2. This study provides evidence that β-arrestin2 may regulate ROS production.

The multicomponent complex NOX catalyzes the conversion of molecular oxygen to ROS [38]. The major producer of intracellular ROS is the NOX4-dependent NADH/NADPH oxidase system, which is the most ubiquitous oxidase system in cells [9]. Compared with WT mice, NOX4 KO mice show significantly less fibrosis after $CCl_4$ injection [27]. However, the role of NOX4 in β-arrestin2 deficiency-mediated ROS inhibition and collagen suppression is not well understood. AngII can cause a large increase in ROS production in HSCs [15]. Therefore, we transfected siRNA targeting NOX4 into LX-2 cells stimulated with AngII. Our results showed that AngII-induced ROS formation was significantly decreased in LX-2 cells treated with NOX4 siRNA, as detected by fluorescence microscopy and flow cytometry of cells labeled with the DCFH-DA fluorescent probe. In addition, downregulation of NOX4 decreased the expression of α-SMA (an activated HSC marker) and collagen I in HSCs. These data indicate that NOX4 might play an important role

in hepatic fibrosis and ROS formation. In the present study, both Western blotting and double immunofluorescence staining showed that NOX4 expression in *Arrb2* KO mice was lower than that in fibrotic WT mice. Furthermore, in vitro depletion and overexpression experiments showed that overexpression of β-arrestin2 increased NOX4 levels in LX-2 cells, while downregulation of β-arrestin2 decreased NOX4 and collagen I expression. These data indicate that knockdown of β-arrestin2 alleviates the elevation of ROS levels in liver fibrosis, probably by modulating NOX4.

β-Arrestin2 is a negative regulator of GPCR signaling and is involved in desensitization and receptor internalization [29]. In addition to potently terminating G-protein signaling, β-arrestin2 can also act as a scaffold for many signaling molecules [39]. Evidence suggests that β-arrestin2 contributes to a series of cellular responses, including cell proliferation, differentiation, and collagen synthesis, by activating the ERK [40] and JNK [41] pathways. Additionally, the ERK and JNK pathways also participate in the regulation of NOX4. For example, according to the literature, ursolic acid regulates the activity and expression of NOX4 by modulating the ERK signaling pathway in HSCs [42]. In palmitic acid-treated AML-12 cells, induction of NOX4 by excessive activation of JNK signaling leads to oxidative stress [43]. Consequently, we investigated whether β-arrestin2 regulates NOX4 expression and ROS production in hepatic fibrosis via the ERK and JNK signaling pathways. For this purpose, we transfected β-arrestin2 overexpression plasmid or β-arrestin2 siRNA into HSCs in vitro. The results demonstrated that overexpression of β-arrestin2 promoted the activation of the ERK and JNK pathways, and that inhibition of ERK and JNK effectively blocked the upregulation of NOX4 and ROS in β-arrestin2-overexpressing LX-2 cells. Conversely, p-ERK and p-JNK expression was decreased in cells that were transfected with β-arrestin2 siRNA, and this decrease was accompanied by decreased NOX4 and ROS levels. Corroborating the results of the in vivo experiments, β-arrestin2 deficiency inhibited NOX4 expression and ROS production. These findings raise the possibility that β-arrestin2 deficiency suppresses NOX4 expression through inhibiting the ERK and JNK signaling pathways, thereby reducing ROS production and ameliorating liver fibrosis.

In summary, we provide evidence that β-arrestin2 may act through ERK and JNK signaling to promote NOX4 expression and ROS production. The results of this study show that β-arrestin2 is essential for regulating ROS production. The pleiotropic functions of β-arrestin2 make precisely targeting this protein of paramount importance. Future studies on the relationship between β-arrestin2 dysregulation and liver fibrosis may provide a conceptual framework for the development of drugs for fibrotic diseases.

## ACKNOWLEDGEMENTS

This work was supported by grants from the National Natural Science Foundation of China (Nos. 81770605 and 81300332) and the program for Young Excellent Talents in Universities of Anhui Province (No. gxyqZD2018024). The authors acknowledge the help of staff members from the Institute of Clinical Pharmacology, Anhui Medical University in conducting these studies.

## AUTHOR CONTRIBUTIONS

WYS and WW designed the research; JCS, JJD, NL, and XQL performed the research, under the supervision of WYS and WW; JJD and JCS analyzed the data; JJD and NL wrote the paper; and WYS revised the paper. All authors have read and approved the final paper.

## ADDITIONAL INFORMATION

**Competing interests:** The authors declare no competing interests.

## REFERENCES

1. Gu YJ, Sun WY, Zhang S, Li XR, Wei W. Targeted blockade of JAK/STAT3 signaling inhibits proliferation, migration and collagen production as well as inducing the apoptosis of hepatic stellate cells. Int J Mol Med. 2016;38:903–11.
2. Chow MD, Lee YH, Guo GL. The role of bile acids in nonalcoholic fatty liver disease and nonalcoholic steatohepatitis. Mol Asp Med. 2017;56:34–44.
3. Ren L, Qi K, Zhang L, Bai Z, Ren C, Xu X, et al. Glutathione might attenuate cadmium-induced liver oxidative stress and hepatic stellate cell activation. Biol Trace Elem Res. 2019;191:443–52.
4. Bouabout G, Ayme-Dietrich E, Jacob H, Champy MF, Birling MC, Pavlovic G, et al. NOX4 genetic inhibition in experimental hypertension and metabolic syndrome. Arch Cardiovasc Dis. 2018;111:41–52.
5. Huang C, Gan D, Luo F, Wan S, Chen J, Wang A, et al. Interaction mechanisms between the NOX4/ROS and RhoA/ROCK1 signaling pathways as new anti-fibrosis targets of ursolic acid in hepatic stellate cells. Front Pharmacol. 2019;10:431.
6. Tarafdar A, Pula G. The role of NADPH oxidases and oxidative stress in neurodegenerative disorders. Int J Mol Sci. 2018;19:3824.
7. Cheng Q, Li C, Yang CF, Zhong YJ, Wu D, Shi L, et al. Methyl ferulic acid attenuates liver fibrosis and hepatic stellate cell activation through the TGF-beta1/Smad and NOX4/ROS pathways. Chem Biol Interact. 2019;299:131–9.
8. Paik YH, Iwaisako K, Seki E, Inokuchi S, Schnabl B, Osterreicher CH, et al. The nicotinamide adenine dinucleotide phosphate oxidase (NOX) homologues NOX1 and NOX2/gp91(phox) mediate hepatic fibrosis in mice. Hepatology. 2011;53:1730–41.
9. Crosas-Molist E, Fabregat I. Role of NADPH oxidases in the redox biology of liver fibrosis. Redoxbiol. 2015;6:106–11.
10. Seo SK, Kim N, Lee JH, Kim SM, Lee SY, Bae JW, et al. Beta-arrestin2 affects cardiac progenitor cell survival through cell mobility and tube formation in severe hypoxia. Korean Circ J. 2018;48:296–309.
11. DeWire SM, Ahn S, Lefkowitz RJ, Shenoy SK. Beta-arrestins and cell signaling. Annu Rev Physiol. 2007;69:483–510.
12. Sun WY, Song Y, Hu SS, Wang QT, Wu HX, Chen JY, et al. Depletion of beta-arrestin2 in hepatic stellate cells reduces cell proliferation via ERK pathway. J Cell Biochem. 2013;114:1153–62.
13. Sun JC, Du JJ, Li XQ, Li N, Wei W, Sun WY. Depletion of β-arrestin 2 protects against $CCl_4$-induced liver injury in mice. Biochem Biophys Res Commun. 2020;522:485–91.
14. Sun WY, Sun JC, Li XR, Peng WT, Wei W. Breeding and genotype identification of *Arrb2* gene knockout mice. Chin Pharmacol Bull. 2018;34:878–81.
15. Cai S, Yang R, Li Y, Ning Z, Zhang L, Zhou G, et al. Angiotensin-(1–7) improves liver fibrosis by regulating the NLRP3 inflammasome via redox balance modulation. Antioxid Redox Signal. 2016;24:795–812.
16. Cherukula K, Nurunnabi M, Jeong YY, Lee YK, Park IK. A targeted graphene nanoplatform carrying histamine dihydrochloride for effective inhibition of leukemia-induced immunosuppression. J Biomater Sci Polym Ed. 2018;29:734–49.
17. Koul M, Kumar A, Deshidi R, Sharma V, Singh RD, Singh J, et al. Cladosporol A triggers apoptosis sensitivity by ROS-mediated autophagic flux in human breast cancer cells. BMC Cell Biol. 2017;18:26.
18. Bankoglu EE, Tschopp O, Schmitt J, Burkard P, Jahn D, Geier A, et al. Role of PTEN in oxidative stress and DNA damage in the liver of whole-body PTEN haplodeficient mice. PLoS One. 2016;11:e166956.
19. Zhou H, Yang R, Wang W, Xu F, Xi Y, Brown RA, et al. Fc-apelin fusion protein attenuates lipopolysaccharide-induced liver injury in mice. Sci Rep. 2018;8:11428.
20. Gharbia S, Balta C, Herman H, Rosu M, Váradi J, Bácskay I, et al. Enhancement of silymarin anti-fibrotic effects by complexation with hydroxypropyl (HPBCD) and randomly methylated (RAMEB) β-cyclodextrins in a mouse model of liver fibrosis. Front Pharmacol. 2018;9:883.
21. Yoshiji H, Kuriyama S, Miyamoto Y, Thorgeirsson UP, Gomez DE, Kawata M, et al. Tissue inhibitor of metalloproteinases-1 promotes liver fibrosis development in a transgenic mouse model. Hepatology. 2000;32:1248–54.
22. Tang N, Zhang YP, Ying W, Yao XX. Interleukin-1β upregulates matrix metalloproteinase-13 gene expression via c-Jun N-terminal kinase and p38 MAPK pathways in rat hepatic stellate cells. Mol Med Rep. 2013;8:1861–5.
23. Zhang X, Feng M, Liu X, Bai L, Kong M, Chen Y, et al. Persistence of cirrhosis is maintained by intrahepatic regulatory T cells that inhibit fibrosis resolution by regulating the balance of tissue inhibitors of metalloproteinases and matrix metalloproteinases. Transl Res. 2016;169:67–79.
24. Sharma M, Arbabzada N, Flood PM. Mechanism underlying beta2-AR agonist-mediated phenotypic conversion of LPS-activated microglial cells. J Neuroimmunol. 2019;332:37–48.
25. Hernández-Aquino E, Zarco N, Casas-Grajales S, Ramos-Tovar E, Flores-Beltrán RE, Arauz J, et al. Naringenin prevents experimental liver fibrosis by blocking TGFβ-Smad3 and JNK-Smad3 pathways. World J Gastroenterol. 2017;23:4354–68.

26. Zhao Y, Ma X, Wang J, He X, Hu Y, Zhang P, et al. Curcumin protects against $CCl_4$-induced liver fibrosis in rats by inhibiting HIF-1α through an ERK-dependent pathway. Molecules. 2014;19:18767–80.
27. Lan T, Kisseleva T, Brenner DA. Deficiency of NOX1 or NOX4 prevents liver inflammation and fibrosis in mice through inhibition of hepatic stellate cell activation. PLoS One. 2015;10:e129743.
28. Iredale JP, Thompson A, Henderson NC. Extracellular matrix degradation in liver fibrosis: biochemistry and regulation. Biochim Biophys Acta. 2013;1832:876–83.
29. Gu YJ, Sun WY, Zhang S, Wu JJ, Wei W. The emerging roles of beta-arrestins in fibrotic diseases. Acta Pharmacol Sin. 2015;36:1277–87.
30. Lovgren AK, Kovacs JJ, Xie T, Potts EN, Li Y, Foster WM, et al. Beta-arrestin deficiency protects against pulmonary fibrosis in mice and prevents fibroblast invasion of extracellular matrix. Sci Transl Med. 2011;3:74ra23.
31. Quack I, Woznowski M, Potthoff SA, Palmer R, Konigshausen E, Sivritas S, et al. PKC alpha mediates beta-arrestin2-dependent nephrin endocytosis in hyperglycemia. J Biol Chem. 2011;286:12959–70.
32. Kim J, Zhang L, Peppel K, Wu JH, Zidar DA, Brian L, et al. Beta-arrestins regulate atherosclerosis and neointimal hyperplasia by controlling smooth muscle cell proliferation and migration. Circ Res. 2008;103:70–9.
33. Cong M, Liu T, Wang P, Fan X, Yang A, Bai Y, et al. Antifibrotic effects of a recombinant adeno-associated virus carrying small interfering RNA targeting TIMP-1 in rat liver fibrosis. Am J Pathol. 2013;182:1607–16.
34. Shi H, Shi A, Dong L, Lu X, Wang Y, Zhao J, et al. Chlorogenic acid protects against liver fibrosis in vivo and in vitro through inhibition of oxidative stress. Clin Nutr. 2016;35:1366–73.
35. Schieber M, Chandel NS. ROS function in redox signaling and oxidative stress. Curr Biol. 2014;24:R453–62.
36. Yadav D, Hertan HI, Schweitzer P, Norkus EP, Pitchumoni CS. Serum and liver micronutrient antioxidants and serum oxidative stress in patients with chronic hepatitis C. Am J Gastroenterol. 2002;97:2634–9.
37. Yang KL, Chang WT, Hong MY, Hung KC, Chuang CC. Prevention of TGF-beta-induced early liver fibrosis by a maleic acid derivative anti-oxidant through suppression of ROS, inflammation and hepatic stellate cells activation. PLoS One. 2017;12:e174008.
38. Andueza A, Garde N, Garcia-Garzon A, Ansorena E, Lopez-Zabalza MJ, Iraburu MJ, et al. NADPH oxidase 5 promotes proliferation and fibrosis in human hepatic stellate cells. Free Radic Biol Med. 2018;126:15–26.
39. Sun YY, Zhao YX, Li XF, Huang C, Meng XM, Li J. Beta-arrestin 2 promotes hepatocyte apoptosis by inhibiting AKT pathway in alcoholic liver disease. Front Pharmacol. 2018;9:1031.
40. Manson ME, Corey DA, Rymut SM, Kelley TJ. Beta-arrestin-2 regulation of the cAMP response element binding protein. Biochemistry. 2011;50:6022–9.
41. McDonald PH, Chow CW, Miller WE, Laporte SA, Field ME, Lin FT, et al. Beta-arrestin 2: a receptor-regulated MAPK scaffold for the activation of JNK3. Science. 2000;290:1574–7.
42. He W, Shi F, Zhou ZW, Li B, Zhang K, Zhang X, et al. A bioinformatic and mechanistic study elicits the antifibrotic effect of ursolic acid through the attenuation of oxidative stress with the involvement of ERK, PI3K/Akt, and p38 MAPK signaling pathways in human hepatic stellate cells and rat liver. Drug Des Devel Ther. 2015;9:3989–4104.
43. Ji JF, Jiao WZ, Cheng Y, Yan H, Su F, Chi LL. ShenFu preparation protects AML12 cells against palmitic acid-induced injury through inhibition of both JNK/NOX4 and JNK/NFkappaB pathways. Cell Physiol Biochem. 2018;45:1617–30.